NUMERICAL INVESTIGATION OF THE PERFORMANCE OF PERFORATED BAFFLES IN A PLATE-FIN HEAT EXCHANGER

by

Houari AMEUR[a*], Djamel SAHEL[b], and Younes MENNI[c]

[a] Department of Technology, University Centre of Naama (Ctr Univ Naama), Naama, Algeria
[b] Department of Technical Sciences, University Amar Thilidji of Laghouat, Laghouat, Algeria
[c] Unite of Research on Materials and Renewable Energies – URMER, Department of Physics, Abou Bekr Belkaid University, Tlemcen, Algeria

Original scientific paper
https://doi.org/10.2298/TSCI190316090A

The present paper is a numerical investigation on the performance of perforated baffles in a plate-fin heat exchanger. Two types of perforations are studied, namely the circular and elliptical shapes. Values of heat transfer coefficient, pressure drop, and thermal performance factor are determined for both cases and compared with those for a smooth channel. Also, the flow fields and heat transfer characteristics are determined for different fluids and various Reynolds numbers. The working fluids are complex, non-Newtonian and have an inelastic shear thinning behavior. The obtained results showed a good enhancement in the thermal performance factor by the suggested design in baffles. In the case of low viscous fluids, the elliptical perforated baffle performs better (by about 63.4%) than the circular one for all values of Reynolds number. But for highly viscous fluids, the elliptical perforation shows higher thermal performance than the circular hole by about 25% for low Reynolds numbers and 27% for high Reynolds numbers. The overall thermal performance factors are about 1.55 and 1.74 for the circular and elliptical perforations, respectively.

Key words: *plate-fin heat exchanger, perforated baffle, non-newtonian fluid, shear thinning fluid, CFD*

Introduction

Plate-fin heat exchangers (PFHE) are highly encountered in different industrial applications such as in air conditioning, refrigeration, heating and other processes. The high performance, low cost, low weight and small size are the main criteria to be controlled during the design and production of this type of heat exchangers. The enhancement of heat transfer rates in such devices may be obtained by various techniques and the baffling technique which is widely used has proven its efficiency [1-3]. The insert of baffles, known as vortex generators (VG) disturbs the fluid-flows and creates swirling vortices, resulting thus in a great exchange between the fluid particles inside the heat exchanger [4-7].

Some studies have been achieved regarding the performance of VG in PFHE. Among others, Wen *et al.* [8] investigated by experiments and numerical simulations the flow patterns in the entrance of a PFHE. In another work, these authors [9] optimized four parameters (the fin thickness, fin height, fin space and interrupted length) of serrated fins in a PFHE. Their optimized configuration allowed an increase in the heat transfer rate by 145 W and a decrease in power consumption by 48.5%. For a PFHE with a triangular channel cross-section, Samadifar

* Corresponding author, e-mail: houari_ameur@yahoo.fr

and Toghraie [10] studied the effect of six different shapes of VG including a simple rectangular, angular rectangular, rectangular trapezius, intended, Wishbone and wavy. They observed that the simple rectangular VG increases the heat transfer of PFHE more than the other models. Based on the corrugated plate-fin (CPF) and the vortex-generator plate-fin (VGPF) configurations, Khoshvaght-Aliabadi *et al.* [11] designed a new corrugated/vortex-generator plate-fin (CVGPF). The CVGPF channel has provided the best thermal-hydraulic performances, followed by the CPF and VGPF channels, respectively. Ma *et al.* [12] investigated the influence of longitudinal vortex generators (LVG) on the performance of a thermoelectric power generator (TEG) with a PFHE. In a comparison with a TEG with smooth channel, they found an increase by 41-75% in the heat input and open circuit voltage of the TEG with LVG.

Although the great enhancement in thermal transfer rates given by VG, there are some negative results such as the high pressure drop and the presence of low heat transfer area behind the baffles. These issues may be overcome by using perforated baffles [13-18]. Some researchers explored the performance of various types of VG with perforations. Among others, Chamoli [19] studied by experiments the heat transfer in a rectangular channel having V-down perforated baffles and his results showed a considerable enhancement in thermal transfer rates. Ary *et al.* [20] investigated the effect of number of holes on the thermal-hydraulic characteristics and they reported that two perforated baffles perform better that one baffle. The thermal efficiency may be increased with the rise of number of holes in perforated circular rings, as reported by Sheikholeslami *et al.* [21].

For a perforated baffle, Sahel *et al.* [22] explored numerically the effect of position of hole which is known as pores axis ratio (PAR), and the best performance was found with the case $PAR = 0.190$. Khoshvaght-Aliabadi *et al.* [23] explored the effects of three passive heat transfer enhancement techniques (nanofluids, winglets, and perforations) on the thermal-hydraulic characteristics of wavy plate fins (WPF). For a perforation diameter equal to 5 mm, they changed the waviness aspect ratios from 0.33-51. Their results revealed that the thermal performance of the winged WPF is significantly superior to that of the other WPF, which is due to the efficient mixing of fluids by the winged design. Compared to the typical WPF, the maximum performance factor of 1.26 is observed for the winged WPF at the highest waviness aspect ratio and the lowest Reynolds number.

Boukhadia *et al.* [24] studied the effect of three shapes of perforation (rectangular, circular, and triangular) in winglet on the performance of PFHE. In comparison with the unbaffled case, the maximum thermal performance factor (TPF) of 2.14 was observed for the circular perforated baffle, followed by the rectangular perforation and then the triangular perforation ($TPF = 1.57$ and 1.46, respectively).

Our search in literature revealed that the perforated baffle is an efficient alternative to eliminate the negative results of the standard baffle. In our knowledge, only one paper [24] has been achieved regarding the effect of perforation shape in baffles for a PFHE. As stated previously, the circular shape of perforation was found more to be efficient than the other shapes studied (rectangular and triangular). Therefore, the main purpose of this paper is to compare between the performance of circular and elliptic perforations in baffles for a PFHE. We are interested about the case of non-Newtonian inelastic shear thinning fluids.

As known, the design of heat exchangers is not an easy task when complex non-Newtonian fluids are involved. This issue concerns primarily chemical and food industries wherein products to be treated may exhibit complex rheological behavior. Also, such fluids as fruit purees and tomato sauces have generally high apparent viscosity, so the cooling inside the exchanger exhibit a complexity [25].

Definition of the problem

A hot complex shear thinning fluid is flowing through a rectangular channel with an inlet temperature T_{in} = 325 K, fig. 1. The wall temperature is fixed at T_w = 266.5 K. We focus in this paper on the cooling of shear thinning fluids and these values of temperature are based on the experimental study performed by Azevedo *et al.* [25], who have studied the same phenomenon for this class of fluids in horizontal pipes.

The length, L, of channel is 300 mm and its width is $A = B$ = 12 mm. The size of each baffle is $a = b$ = 5 mm and the thickness of each one is 1 mm. Six ranges of baffles are inserted and the distance, l, between two consecutives ranges is 20 mm. The effect of baffles with circular/elliptical perforations is investigated. The flow is laminar and Reynolds number is ranging from 0.1 to 300. Further details on geometrical parameters are provided in figs. 1(a) and 1(b).

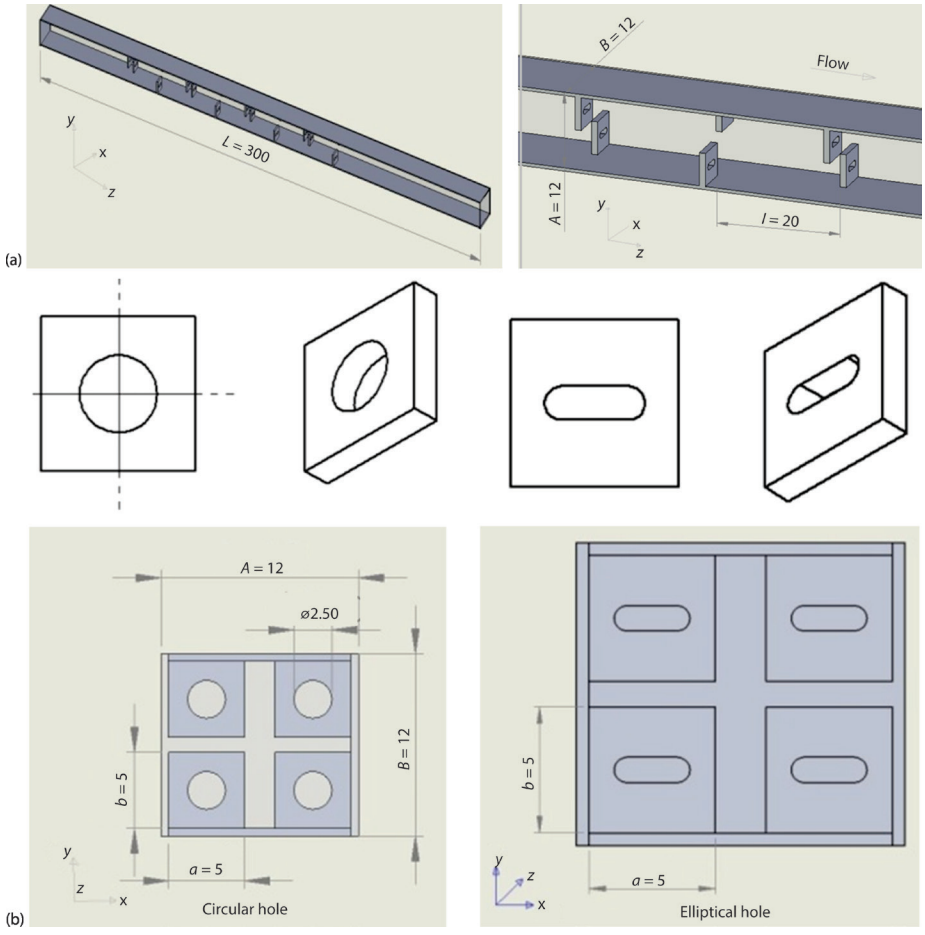

Figure 1. Simulated geometry (a) and different shapes of perforated baffles studied (b)

Two complex non-Newtonian fluids have been used as working fluids, namely the carboxy methyl cellulose (CMC) solution, with the flow behavior index n = 0.69 and the consistency index m = 0.02 Pa s^n) and the Ketrol solution. The rheological properties of the Ketrol solutions considered in this paper are summarized in tab. 1.

Table 1. Rheological properties of the Ketrol solutions

Solution No.	1	2	3	4	5
n [–]	0.80	0.71	0.68	0.64	0.56
m [Pa·s^n]	9.5	16.5	23.6	34	74.8

Theoretical background

The flow in the channel is continuous, laminar and steady-state and the heat transfer is natural. The working fluid has a shear thinning behavior modeled by the Ostwald law:

$$\tau = m\dot{\gamma}^n \tag{1}$$

$$\eta = m\dot{\gamma}^{n-1} \tag{2}$$

where τ is the shear stress, $\dot{\gamma}$ – the shear rate, and η – the apparent viscosity.

Based on the aforementioned assumptions, the governing equations are written:

– Conservation of mass

$$\frac{\partial}{\partial x_i}\left(\rho u_\mathrm{i}\right) = 0 \tag{3}$$

– Conservation of momentum

$$\frac{\partial}{\partial x_\mathrm{i}}\left(\rho u_\mathrm{i} u_\mathrm{k}\right) = \frac{\partial}{\partial x_\mathrm{i}}\left(\mu_\mathrm{a}\frac{\partial u_\mathrm{k}}{\partial x_\mathrm{i}}\right) - \frac{\partial p}{\partial x_\mathrm{k}} \tag{4}$$

– Conservation of energy

$$\frac{\partial}{\partial x_\mathrm{i}}\left(\rho u_\mathrm{i} T\right) = \frac{\partial}{\partial x_\mathrm{i}}\left(\frac{k_\mathrm{f}}{C_p}\frac{\partial T}{\partial x_\mathrm{i}}\right) \tag{5}$$

where C_p is the specific heat of working fluids.

The heat transfer rate and the pressure are determined by using the Colburn factor, j, and the Fanning friction factor, f, respectively:

$$j = \frac{h}{\rho u C_p}\mathrm{Pr}^{2/3} \tag{6}$$

$$f = \frac{2\Delta P}{\rho u^2}\frac{D_\mathrm{h}}{L} \tag{7}$$

where Pr is the Prandtl number, C_p – the specific heat of fluid, ρ – the fluid density, u – the velocity, C_p – the specific heat of working fluids, L – the channel length, D_h – the hydraulic diameter, ΔP – the pressure difference between inlet and outlet, and h – the convective heat transfer coefficient which is defined:

$$h = \frac{Q_\mathrm{conv}}{S\left(T_\mathrm{w} - T_b\right)_\mathrm{LMTD}} \tag{8}$$

$$Q_\mathrm{conv} = \dot{m}C_p\left(T_{b,\mathrm{out}} - T_{b,\mathrm{in}}\right) \tag{9}$$

where S is the heat transfer area, $\dot{m}$ – the mass-flow rate, $T_{b,\mathrm{in}}$ and $T_{b,\mathrm{out}}$ are the average temperature of fluid at the inlet and outlet, respectively, and $(T_\mathrm{w} - T_b)_\mathrm{LMTD}$ – the log mean temperature difference:

$$\left(T_{\mathrm{w}} - T_b\right)_{\mathrm{LMTD}} = \frac{\Delta T_{\mathrm{w}-b,\mathrm{in}} - \Delta T_{\mathrm{w}-b,\mathrm{out}}}{\log\left(\dfrac{\Delta T_{\mathrm{w}-b,\mathrm{in}}}{\Delta T_{\mathrm{w}-b,\mathrm{out}}}\right)} \tag{10}$$

where $\Delta T_{\mathrm{w}\text{-}b,\ \mathrm{in}}$ and $\Delta T_{\mathrm{w}\text{-}b,\ \mathrm{out}}$ are the difference in temperatures at the inlet and outlet sections between the wall and the bulk fluid.

For a shear thinning fluid, the Reynolds number is given:

$$\mathrm{Re} = \frac{\rho u_{\mathrm{in}}^{2-n} D_{\mathrm{h}}^{n}}{m}\left(\frac{3n+1}{4n}\right)^{n} 8^{1-n} \tag{11}$$

In dimensionless form, we define the axial, transversal and vertical co-ordinates:

$$X^* = X/D_{\mathrm{h}},\ Y^* = Y/D_{\mathrm{h}},\ Z^* = Z/D_{\mathrm{h}}$$

Numerical method

At present, there are a number of 3-D industrial codes that allow the prediction of fluid-flows by solving the Navier-Stokes equations using the finite volume method. In this study, all investigations are carried out by ANSYS CFX16.0 code, using the tetrahedral mesh type to achieve geometry simulation. The geometry and mesh are created by the computer tool ANSYS ICEM CFD (version 16.0).

In the present paper, the cooling of complex non-Newtonian fluids through rectangular channels is explored. These fluids are usually encountered in industrial processes under low Reynolds numbers [25]. So, the convective heat transfer is studied under laminar flow conditions. The boundary conditions of the computational geometry are given:

– Inlet condition: at the channel inlet

$$u_y = u_z = 0,\ u_x = u_{\mathrm{in}} = \text{constant},\ T = T_{\mathrm{in}} = 325\ \mathrm{K} \tag{12}$$

we note that the value of u_{in} is defined by eq. (11) according to the given Reynolds number, where Re = 1-300.

– Outlet condition: a zero gauge pressure is set at the channel exit
– Symmetry condition: for the right and left sides

$$u_x = u_y = u_z = 0,\ \frac{\partial T}{\partial x} = 0 \tag{13}$$

– Wall condition: for the lower and upper surfaces

$$u_x = u_y = u_z = 0,\ T = T_{\mathrm{w}} = 266.5\ \mathrm{K},\ \frac{\partial T}{\partial z} = 0 \tag{14}$$

– Baffles: are considered as adiabatic walls.

In order to capture the details of the thermal and hydrodynamic boundary-layers, the density of mesh was increased near the walls of channel and baffles. On the baffle edge, the number of nodes was increased enough to define the curvature of the perforation in baffles. Mesh tests (M) were performed by checking that additional cells did not give a variation in the performance factor $(j/f)/(j/f)_{\mathrm{unbaffled}}$ by more than 2.5%, tab. 2.

This grid independency was achieved by increasing the number of grids by a factor of about 2. The original mesh of the computational geometry had about 205123 cells. Then, this number was increased until 410246 cells. This new mesh has given a variation in the perfor-

Table 2. Details on the grid independency test

	M_1	M_2	M_3	M_4
Number of cells	205123	410246	920458	1700526
$(j/f)/(j/f)_{unbaffled}$	1.31981	1.28505	1.27311	1.27366
Time required [s]	7526	12598	21589	35589

mance factor by more than 3%. Thus, it was increased until 0.9 million and then to 1.7 million of cells. From the 3rd mesh which contains about 0.9 million of cells, the additional cells did not vary the performance factor by more than 2.5%. Therefore, it was selected to be used in the following calculations. We note that the values of performance factor reported in tab. 2 concerns the case of a circular perforated baffle, for the solution No. 5 and Re = 100.

The second order central difference scheme was used to approximate the diffusion term in the momentum and energy equations. This scheme is known by its stable solution. For the discretization of convection terms, a second-order upwind scheme was used. The Navier-Stockes governing equations were solved by a segregated implicit iterative scheme. The semi implicit method for pressure linked equation (SIMPLE) scheme was used to perform the velocity-pressure coupling.

The under-relaxation factors 0.3, 0.7, and 0.8 for the pressure, momentum, and energy, respectively, were used to ensure the computational convergence. The residual target for the continuity, momentum and energy equations was 10^{-5}. Most simulations required about 1200-1400 iterations and about 5-6 hours on a computer machine with Intel Core i7 CPU, 8.0 GB of RAM and a clock speed of 2.20 GHz.

Results and discussion

Validation

Our search in the literature showed that the only geometrical configuration which is similar to our work is that of Khoshvaght-Alibadi *et al.* [4]. However, these authors explored the influence of baffle shape (rectangular, triangular, and trapezoidal), but no perforation is inserted in the baffles. In the present paper, we examined the influence of the shape of perforation inserted in a rectangular baffle. Therefore, we have chosen for validation the case of a rectangular baffle as that used by Khoshvaght-Alibadi *et al.* [4]. Values of the heat transfer coefficient depending on Reynolds number are presented in fig. 2. In this figure, our predicted results and those obtained experimentally and numerically by Khoshvaght-Alibadi *et al.* [4] are provided. We note that the working fluid considered in this case is Newtonian (water, Pr = 7) and the baffles are without perforations. As clearly observed, the agreement is satisfactory. Also, our study is achieved within the range of Reynolds number from 1-300, and the validation is done for Reynolds number ranging between 500 and 1900 (*i.e.* in the laminar flow regime). So, the numerical method is proved to be accurate for the following computations. We remind that, in the pre-processing part of the computer code, we introduce the eq. (2). When $n = 1$, it corresponds to the Newtonian behavior of fluid.

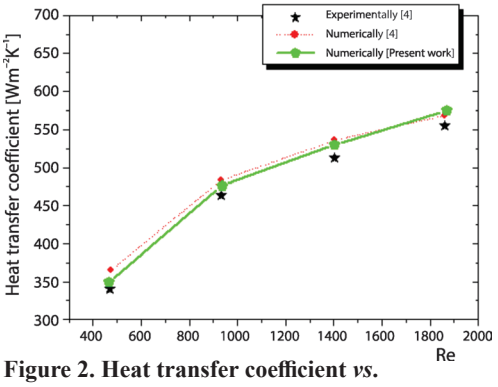

Figure 2. Heat transfer coefficient *vs.* Reynolds number (validation)

Thermal and hydrodynamic behaviors

It is known that the flow of viscous fluids in channels is characterized by the formation of thermal and hydrodynamic boundary-layers near the wall of channel due to the viscous forces. Figure 3 shows the formation of hydrodynamic boundary-layer in the smooth channel (1st slice) and the effect of the presence of perforated baffles on this boundary (2nd and 3rd slices). For the baffled channel, the streamlines are presented on the vertical plane passing by $Z^* = 0.29$ (*i.e.* through the perforation). The presence of baffles inside the channel helps to destruct the hydrodynamic boundary-layer and creates intensified turbulence and velocity fluctuations near the walls. But, the major problem in using these baffles is the formation stagnated regions behind them. Therefore, an attempt is made here to overcome this issue by using the technique of perforated baffles. Two shapes of perforations were used, namely: circular and elliptical shapes.

Figure 4 shows the streamlines under a 3-D view. This figure depicts a supplementary comprehension of the effect of the perforated space on the reduction of dead zones in the downstream region of baffles. As observed, the elliptical perforation provides a highly intense agitation of fluid particles and enlarged swirling flow, compared to the circular shape of perforation in baffles.

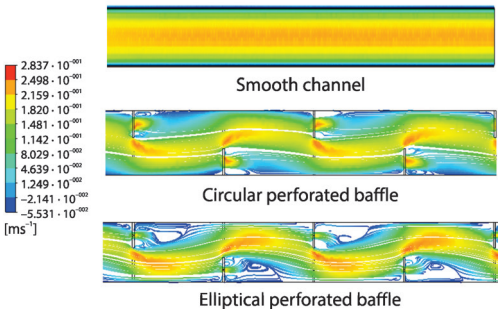

Figure 3. Streamlines for CMC solution, Re = 100, at $Z^* = 0.29$ (through the perforation)

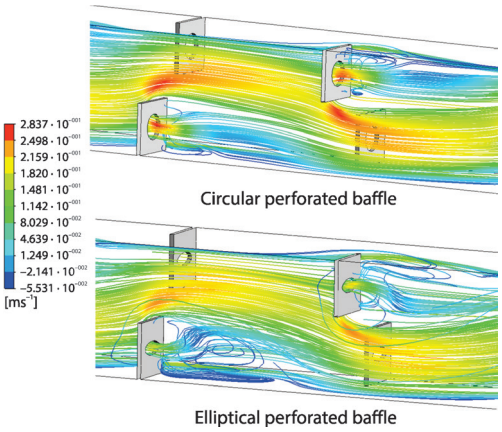

Figure 4. The 3-D Streamlines for CMC solution, Re = 100

Habitually, there is a fundamental relation between the formation of the hydrodynamic and thermal boundary-layers, where the flow structures influence directly on the thermal execution inside the channel [26-29]. Figures 5 and 6 show the distribution of temperature along the channel, under a 2-D and 3-D views, respectively. In these figures, the formation of thermal boundary-layer is appear clearly in the case of a smooth channel. The formation of hot points behind the baffles is a result of the formation of stagnated zones in these regions. Thus, for the thermal aspect, the formation of hot points downstream of baffles is another

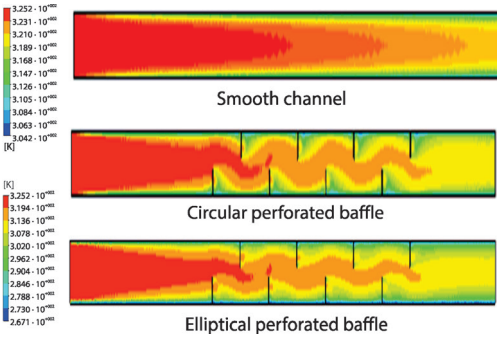

Figure 5. Temperature distribution for CMC solution, Re = 100, at $Z^* = 0.29$ (through the perforation)

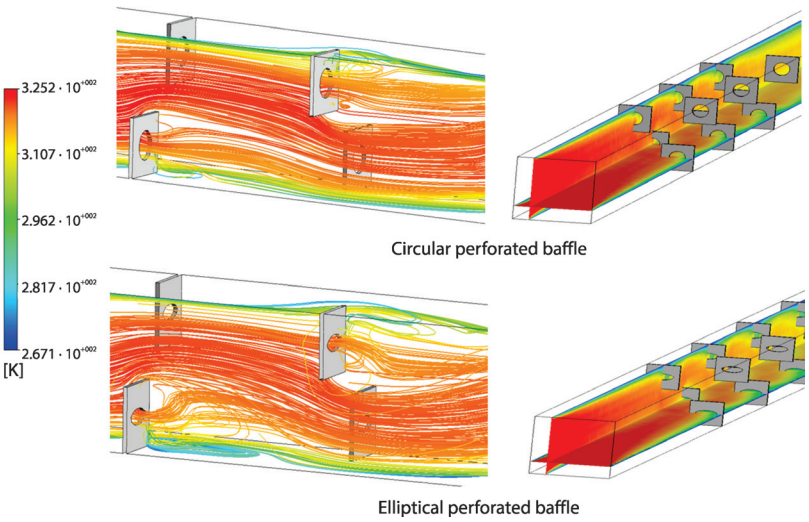

Figure 6. The 3-D thermal fields for CMC solution, Re = 100

problem which reduces the heat transfer execution in these regions. Therefore, the presence of elliptical and circular perforated baffles can diminish the formation of hot points by means of agitation mechanism of the stagnated zones, and as a result it increases the heat transfer coefficients. In a comparison between the two shapes of perforations, it seems that the length in channel to achieve the disered cooling of fluid is smaller in the case of elliptical perforated baffles that that with circular perforation.

Reynolds number is another important physical parameter to enhance the heat transfer execution in thermal systems. The Reynolds number is introduced in term of channel inlet velocity, where the augmentation of the inlet velocity increases the fluctuation of velocity near the walls of channel. Figure 7 depicts the effect of Reynolds numbers on the flow structure inside the baffled channel. The increase of Reynolds numbers augments proportionally the size of the re-circulation loops formed at the extremity of baffle and it intensifies the vortex flow upstream and downstream of baffles. Also, the stagnated zones behind the baffles tend to disappear with the increases of Reynolds number values. This mechanism is considered as an advantage to reduce the formation of lower heat transfer areas.

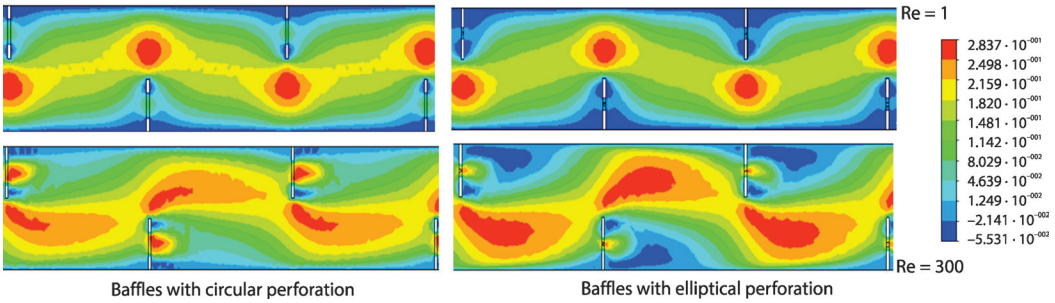

Figure 7. Axial velocity for CMC solution, at $Z^* = 0.29$ (through the perforation)

Heat transfer

As we explain previous, the presence of baffles helps to destruct the development of the thermal and hydrodynamic boundary-layers. Figure 8 illustrates the variation of heat transfer coefficients *vs.* Reynolds numbers values. We can clearly report that the heat transfer coefficients augment with the increases of Reynolds numbers due to the intensification of turbulence and velocity fluctuations near the wall. In addition, the location of the perforated space on baffles as elliptical and circular forms presents supplementary configurations which help the passage of fluid particles through the pores and agitate the stagnated zones behind the baffles. However, the elliptical perforated baffle allows higher values of heat transfer coefficients compared to the circular shape. At the highest Reynolds number value (Re = 300) and for the elliptical and circular shapes, the values of heat transfer coefficients are about 5 and 4 times compared to channel without baffles, respectively.

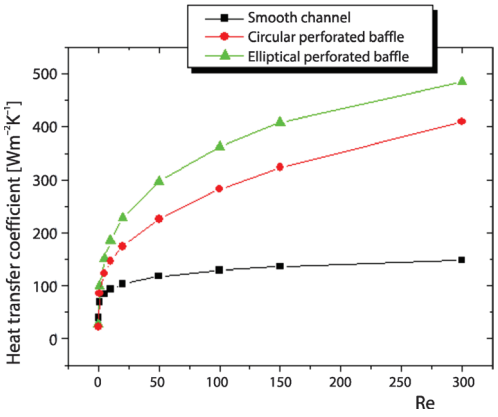

Figure 8. Heat transfer coefficient for CMC solution

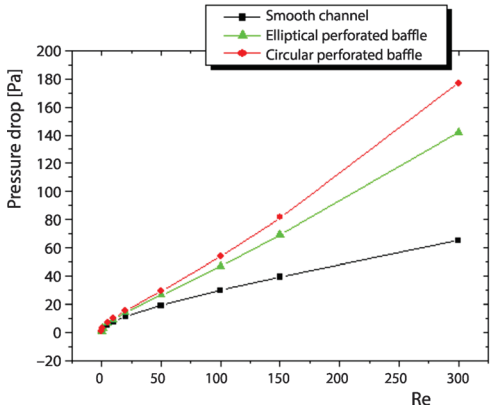

Figure 9. Pressure drop for CMC solution

Pressure drop

Like all geometrical configurations in literature, the augmentation of heat transfer coefficients in the baffled channels is accompanied by a penalty in the pressure drop. For the arrangements studied in the present work, the variation of pressure drop *vs.* Reynolds numbers is shown in fig. 9. In this figure, the pressure drop increases with the rise of Reynolds number. This is due to the changes in flow direction and the generated vortex near the walls and baffles. In comparison between the perforated baffles, the elliptical shape ensures better heat transfer coefficient and creates a minimum pressure drop penalty, compared to the circular perforated baffles. At Re = 300 and in comparison with the channel without baffles, the pressure drop values are about 2.5 and 3 times for elliptical and circular perforated baffles, respectively.

Thermal performances evaluation

The performance factor, j/f, is used in this paper to determine the overall performance in terms of heat transfer rates and pressure drops. The predicted results of performance factor are depicted on fig. 10 for different Reynolds number and various geometrical configurations. As observed, the increase of Reynolds number yields a considerable increase in the performance factor until Re = 150 where the performance factor remains almost constant for this kind of fluids.

In terms of higher performance factor, the comparison between all cases studied allows the following classification: a channel with elliptical perforated baffle > a channel with

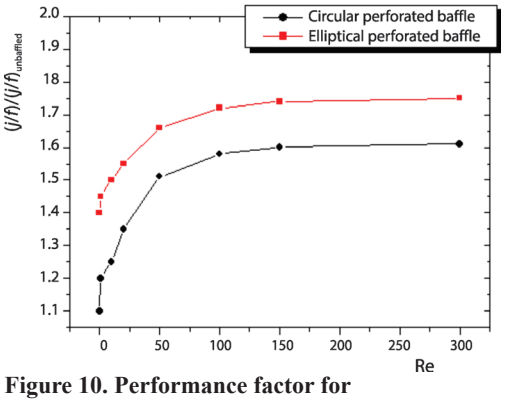

Figure 10. Performance factor for CMC solution

circular perforated baffle > unbaffled channel. Compared to the smooth channel and for Reynolds numbers up to 150, the performance factors for elliptical and circular perforations are higher by about 77% and 13.6% than that for unbaffled channel. Therefore, the elliptical shape merits to be used in the design of thermal systems with low viscous fluids.

The comparison between the elliptical and circular perforations reveals the superiority of elliptical perforation in terms of enhancement in heat transfer with only a slight difference in pressure drop. There is a relatively small change in geometry, but it leads to large changes in the heat transfer rates. In general, the curved shape of perforation in baffles allows an easy passage of fluid particles through the perforation accompanied with a rotation of fluid, resulting thus in intensified interaction between fluids particles and enhanced heat transfer. However, the elliptical shape of perforation allows an intensified rotation of fluid particles than that provided by the circular perforation. Therefore, the greatest values of heat transfer coefficients are obtained by first case (elliptical).

In other geometrical configurations and especially in finned-tube heat exchangers, many researchers compared between the performance of circular and elliptical tubes and they found that the elliptical shape can offer significant advantages over the circular ones because of smaller wake region and lower profile drag on the air-side [29-31].

Fluid rheology

Many industrial processes, such as food sterilization and well cementing exhibit complex non-Newtonian fluids in channels and the thermal convection of these fluids is of practical importance.

In this paper, we interest to the cooling of non-Newtonian fluids which have an inelastic shear thinning behavior modeled by the Oswald De Wale Law. The Ketrol solutions with various concentrations are used in this section investigate the effect of fluid rheology on the thermo-hydraulic performance of the PFHE. All rheological properties are summarized in tab. 1.

Five cases of different concentrations of the Ketrol solutions are used. We remind that for the power law fluids, when the index n is equal to 1 it corresponds to the Newtonian behavior.

Values of the heat transfer coefficient are depicted on fig. 11 for different solutions and different Reynolds numbers and both types of perforations. At very low Reynolds number (Re = 1), a slight increase in the heat transfer coefficient is observed for the two shapes of perforation. However, this coefficient remains almost constant for all solutions with increased Reynolds number.

The comparison between the two shapes of perforation when changing Reynolds number reveals an interesting remark. The elliptical perforation provides higher heat transfer coefficient than the circular one at low Reynolds number (Re = 1) and *vice versa* with increased Reynolds number (Re = 100).

Finally, the thermal performance factor has been calculated taking into account the fluid properties, flow rates and the shape of perforation in baffles, fig. 12. The three parameters

have shown the following effect: the performance factor increases with increased flow consistency index (from solution No. 1-5) and increased Reynolds number. For highly viscous fluids, the elliptical perforation performs better than the circular one at low Reynolds number (a superiority by about 25% for solution No. 5 at Re = 1). At high Reynolds number, the elliptical shape is found also to be better than the circular one (a superiority by about 27% for solution N° 5 at Re = 100). This is due to the size and shape of perforated space in the elliptical baffle, which allows the passage of more fluid particles through the pore, resulting thus in intensified swirling flows and increased heat transfer area behind the baffle, when compared with the circular perforation.

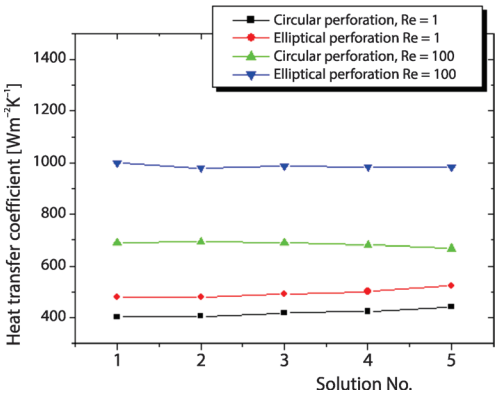

Figure 11. Heat transfer coefficient for different solutions

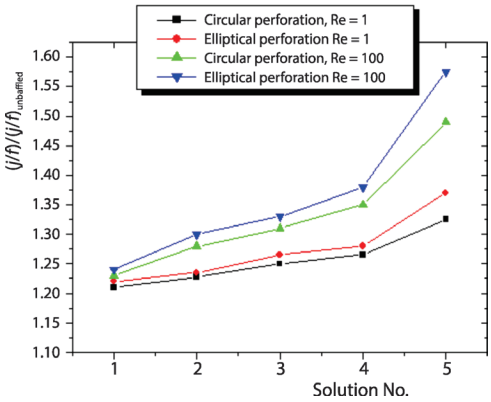

Figure 12. Performance factor for different solutions

Conclusion

The performance of a PFHE for the cooling of complex non-Newtonian fluids has been determined numerically in this paper. The working fluids (CMC and Ketrol solutions) have an inelastic shear thinning behavior. The CMC solution has a low apparent viscosity. However, the five Ketrol solutions used are highly viscous. The thermohydraulic characteristics of the system have been determined for different flow rates, fluid properties and design of perforation in baffles (circular and elliptical shapes).

The mainly finding can be summarized as follows.

- At the highest Reynolds number value (Re = 300), the values of heat transfer coefficients are higher by about 5 and 4 times for the elliptical and circular shapes, respectively, compared with the unbaffled channel.
- Compared with the smooth channel, values of the pressure drop for the elliptical and circular perforated baffles are higher by about 2.5 and 3 times, respectively.
- The perforated baffle has revealed a good enhancement in the thermal performance factor than the unbaffled channel. The overall thermal performance factors are about 1.55 and 1.74 for the circular and elliptical perforations, respectively, over than that for the smooth channel.
- In the case of low viscous fluids, the elliptical perforated baffle performs better than the circular one for all values of Reynolds number.
- For highly viscous fluids (Solution No. 5), the elliptical perforation performs better than the circular one (a superiority by about 25% and 27% at Re = 1 and 100, respectively.

Nomenclature

A – width of channel in X-direction, [m]
a – length of baffle, [m]
B – width of channel in Y-direction, [m]
b – width of baffle, [m]
C_p – specific heat, [J kg^{-1}K^{-1}]
D_h – hydraulic diameter, $D_h = (4LA_c)/A_t$, [m]
f – fanning friction factor
h – effective heat transfer coefficient, [Wm^{-2}K^{-1}]
j – Colburn factor
L – length of channel, [m]
l – distance between two consecutives ranges of baffles, [m]
m – consistency index, [Pa·s^n]
$\dot{m}$ – mass-flow rate, [Kgs^{-1}]
Nu – Nusselt number
n – flow index, [–]
ΔP – pressure drop, [Pa]
Pr – Prandtl number
Q_{conv} – convective heat transfer rate, [W]
Re – Reynolds number
S – surface in contact with working fluid, [m^2]
T – temperature, [K]
T_{in} – inlet temperature, [K]
T_w – wall temperature
$T_{b,in}$, $T_{b,out}$ – average temperature of fluid at the inlet and outlet of test section, [K]
$(T_w - T_b)_{LMTD}$ – log mean temperature difference, [K]
u – mean velocity, [ms^{-1}]
X, Y, Z – axial, transversal and vertical co-ordinates, [m]

Greek symbols

$\dot{\gamma}$ – shear rate, [s^{-1}]
η – apparent viscosity, [kgm^{-1}s^{-1}]
ρ – density, [kgm^{-3}]
τ – shear stress, [Pa]

Acronyms

CPF – corrugated plate-fin
CMC – carboxy methyl cellulose
LVG – longitudinal VG
PAR – pores axis ratio
PHHE – plate-fin heat exchanger
TEG – thermoelectric power generator
TPF – thermal performance factor
VG – vortex generator
VGPF – vortex-generator plate-fin
WPF – wavy plate-fin

References

[1] Khoshvaght-Aliabadi, M., *et al*., Role of Channel Shape on Performance of Plate-Fin Heat Exchangers: Experimental Assessment, *International Journal of Thermal Science*, *79* (2014), May, pp. 183-193
[2] Khoshvaght-Aliabadi, M., *et al*., Experimental Analysis of Thermal-Hydraulic Performance of Copper-Water Nanofluid-Flow in Different Plate-Fin Channels, *Experimental Thermal and Fluid Sciences*, *52* (2014), Jan., pp. 248-258
[3] Ahmed, H. E., *et al*., Heat Transfer Enhancement of Laminar Nanofluids Flow in a Triangular Duct Using Vortex Generator, *Superlattices Microstructures*, *52* (2012), 3, pp. 398-415
[4] Khoshvaght-Aliabadi, M. K., *et al*., Performance of a Plate-Fin Heat Exchanger with Vortex-Generator Channels: 3-D-CFD Simulation and Experimental Validation, *International Journal of Thermal Sciences*, *88* (2015), Feb., pp. 180-192
[5] Alem, K., *et al*., The CFD Investigations of Thermal and Dynamic Behaviors in a Tubular Heat Exchanger with Butterfly Baffles, *Front in Heat and Mass Transfer (FHMT)*, *10* (2018), Mar., 27
[6] Sahel, D., *et al*., A Numerical Study of Fluid-Flow and Heat Transfer over a Fin and Flat Tube Heat Exchangers with Complex Vortex Generators, *European Physical Journal Applied Physics*, *78* (2017), 3, ID34805
[7] Mellal, M., *et al*., Hydro-Thermal Shell-Side Performance Evaluation of a Shell and Tube Heat Exchanger under Different Baffle Arrangement and Orientation, *International Journal of Thermal Sciences*, *121* (2017), Nov., pp. 138-149
[8] Wen, J., *et al*., An Experimental and Numerical Investigation of Flow Patterns in the Entrance of Plate-Fin Heat Exchanger, *International Journal of Heat and Mass Transfer, 49* (2006), 9-10, pp. 1667-1678
[9] Wen, J., *et al*., Optimization Investigation on Configuration Parameters of Serrated Fin in Plate-Fin Heat Exchanger Using Genetic Algorithm, *International Journal of Thermal Sciences*, *101* (2016), Mar., pp. 116-125
[10] Samadifar, M., Toghraie, D., Numerical Simulation of Heat Transfer Enhancement in a Plate-Fin Heat Exchanger Using a New Type of Vortex Generators, *Applied Thermal Engineering*, *133* (2018), Mar., pp. 671-681
[11] Khoshvaght-Aliabadi, M., *et al*., Thermal-Hydraulic Characteristics of Plate-Fin Heat Exchangers with Corrugated/Vortex-Generator Plate-Fin (CVGPF), *Applied Thermal Engineering*, *98* (2016), Apr., pp. 690-701

[12] Ma, T., *et al*., Numerical Study on Thermoelectric-Hydraulic Performance of a Thermoelectric Power Generator with a Plate-Fin Heat Exchanger with Longitudinal Vortex Generators, *Applied Energy*, *185* (2017), Part 2, pp. 1343-1354
[13] Huang, K. D., *et al*., Experimental Study of Fluid-Flow and Heat Transfer Characteristics in the Square Channel with a Perforation Baffle, *International Communications in Heat and Mass Transfer*, *35* (2008), 9, pp. 1106-1112
[14] Karwa, R., Maheshwari, B. K., Heat Transfer and Friction in an Asymmetrically Heated Rectangular Duct with Half and Fully Perforated Baffles at Different Pitches, *International Communications in Heat and Mass Transfer*, *36* (2009), 3, pp. 264-268
[15] Liu, C., *et al*., Experimental Investigation on Liquid-Flow and Heat Transfer in Rectangular Micro-Channel with Longitudinal Vortex Generators, *International Journal of Heat and Mass Transfer*, *54* (2011), 13-14, pp. 3069-3080
[16] Jin, Q., *et al*., Numerical Investigation of Heat Transfer Enhancement in Ribbed Channel for the First Wall of DFLL-TBM in ITER, *Fusion Engineering Design*, *87* (2012), 7-8, pp. 974-978
[17] Farhad-Ismail, M., *et al*., Numerical Investigation of Turbulent Heat Convection from Solid and Longitudinally Perforated Rectangular Fins, *Procedia Engineering*, *56* (2013), Dec., pp. 497-502
[18] Bhuiyan, A. A., *et al*., Numerical Modelling of Thermal Characteristics in a Micro Structure Filled Porous Cavity with Mixed Convection, *International Journal of Heat and Mass Transfer*, *93* (2016), Feb, pp. 464-476
[19] Chamoli, S., Hybrid FAHP (Fuzzy Analytical Hierarchy Process)-FTOPSIS (Fuzzy Technique for Order Preference by Similarity of an Ideal Solution) Approach for Performance Evaluation of the V Down Perforated Baffle Roughened Rectangular Channel, *Energy*, *84* (2015), May, pp. 432-442
[20] Ary, B. K. P., *et al*., The Effect of the Inclined Perforated Baffle on Heat Transfer and Flow Patterns in the Channel, *International Communications in Heat and Mass Transfer*, *39* (2012), 10, pp. 1578-1583
[21] Sheikholeslami, M., *et al*., Experimental Study on Turbulent Flow and Heat Transfer in an Air to Water Heat Exchanger Using Perforated Circularring, *Experimental Thermal and Fluid Sciences*, *70* (2016), Jan., pp. 185-195
[22] Sahel, D., *et al*., Enhancement of Heat Transfer in a Rectangular Channel with Perforated Baffles, *Applied Thermal Engineering*, *101* (2016), May, pp. 156-164
[23] Khoshvaght-Aliabadi, M., *et al*., Thermal-Hydraulic Performance of Wavy Plate-Fin Heat Exchanger Using Passive Techniques: Perforations, Winglets, and Nanofluids, *International Communications in Heat and Mass Transfer*, *78* (2016), Nov., pp. 231-240
[24] Boukhadia, K., *et al*., Effect of the Perforation Design on the Fluid-Flow and Heat Transfer Characteristics of a Plate Fin Heat Exchanger, *International Journal of Thermal Sciences*, *126* (2018), Apr., pp. 172-180
[25] Azevedo, I., *et al*., Laminar Cooling of Pseudoplastic Fluids Flowing through Cylindrical Horizontal Pipes, *International Journal of Heat and Fluid-Flow*, *16* (1995), 2, pp. 125-130
[26] Ameur, H., Sahel, D., Effect of Some Parameters on the Thermo-Hydraulic Characteristics of a Channel Heat Exchanger with Corrugated Walls, *Journal of Mechanical and Energy Engineering*, *3* (2019), 1, pp. 53-60
[27] Ameur, H., Effect of the Baffle Inclination on the Flow and Thermal Fields in Channel Heat Exchangers, *Results in Engineering*, *3* (2019), 100021
[28] Sahel, D., *et al.*, Effect of the Size of Graded Baffles on the Performance of Channel Heat Exchangers, *Thermal Science*, *24* (2018), 2A, pp. 767-775
[29] Leu, J. S., *et al*., A Numerical Investigation of Louvered Fin-and-Tube Heat Exchangers Having Circular and Oval Tube Configurations, *International Journal of Heat and Mass Transfer, 44* (2001), 22, pp. 4235-4243
[30] Chu, P., *et al*., The 3-D Numerical Study on Fin-and-Oval-Tube Heat Exchanger with Longitudinal Vortex Generators, *Applied Thermal Engineering*, *29* (2009), 5-6, pp. 859-876
[31] Sun, L., Zhang, C. L., Evaluation of Elliptical Finned-Tube Heat Exchanger Performance Using CFD and Response Surface Methodology, *International Journal of Thermal Sciences*, *75* (2014), Jan., pp. 45-53

Paper submitted: March 16, 2019
Paper revised: July 26, 2019
Paper accepted: February 4, 2020